3-Dimentional Mapping Coastal Zone using High Resolution Satellite Stereo Imageries

Zhonghua Hong[12*],**Fengling Liu**[1],**Yun Zhang**[1]

1. College of Information Technology, Shanghai Ocean University, 999 Hucheng Huan Road, Shanghai, P. R. China.
2. College of Surveying and Geo-informatics and Research, Tongji University, 1239 Siping Road, Shanghai, P. R. China.

Abstract. The metropolitan coastal zone mapping is critical for coastal resource management, coastal environmental protection, and coastal sustainable development and planning. The results of geometric processing of a Shanghai coastal zone from 0.7-m-resolution QuickBird Geo stereo images are presented firstly. The geo-positioning accuracy of ground point determination with vendor-provided rigorous physical model (RPM) parameters is evaluated and systematic errors are found when compared with ground control points surveyed by GPS real-time kinematic (GPS-RTK) with 5cm accuracy. A bias-compensation process in image space that applies a RPM bundle adjustment to the RPM-calculated 3D ground points to correct the systematic errors is used to improve the geo-positioning accuracy. And then, a area-based matching (ABM) method is used to generated the densely corresponding points of left and right QuickBird images. With the densely matching points, the 3-dimentinal coordinates of ground points can be calculated by using the refined geometric relationship between image and ground points. At last step, digital surface model (DSM) can be achieved automatically using interpolation method. Accuracies of the DSM as assessed from independent checkpoints (ICPs) are approximately 1.2 m in height.

Keywords: metropolitan, coastal zone, 3-dimentional mapping, high resolution satellite stereo imageries.

1. Introduction

The metropolitan coastal zone mapping is critical for coastal resource management, coastal environmental protection, and coastal sustainable development and planning. With the rapid development of high resolution satellite imagery (HRSI), 3-Dimentinal mapping coastal zone become feasibility scheme [6] [8] [10] [11] [13].However, geo-positioning accuracy will serious impact the final accuracy of coastal mapping [1] [8] [9]. Moreover, the vender provided sensor model parameters remain obvious bias [4] [14] [15] when were used to directly geo-positioning. Therefore, the sensor parameters should be refined by ground control points. There are two categories sensor models in HRSI such as: rigorous physical model (RPM) and rational function model (RFM). The RFM

* Corresponding Author. E-mail address: hzh_2000@163.com; zhhong@shou.edu.cn

refinement was presented by many researchers, but the RPM refinement reported few. Another key technology is automatic digital surface model (DSM) generation can be found [2] [12] [16]. Therefore, this paper will discuss the RPM refinement for 3-Dimentional mapping coastal zone using QuickBird stereo images in Shanghai.

2. Methods

Figure 1 shows the entire framework for automatic 3-Dimentional Mapping Coastal Zone using QuickBird stereo HRSI. Two issues are investigated: (1) area-based automatic image matching, and (2) rrigorous physical refinement. The former two key technologies used in this approach will discuss in detailed in the following sections.

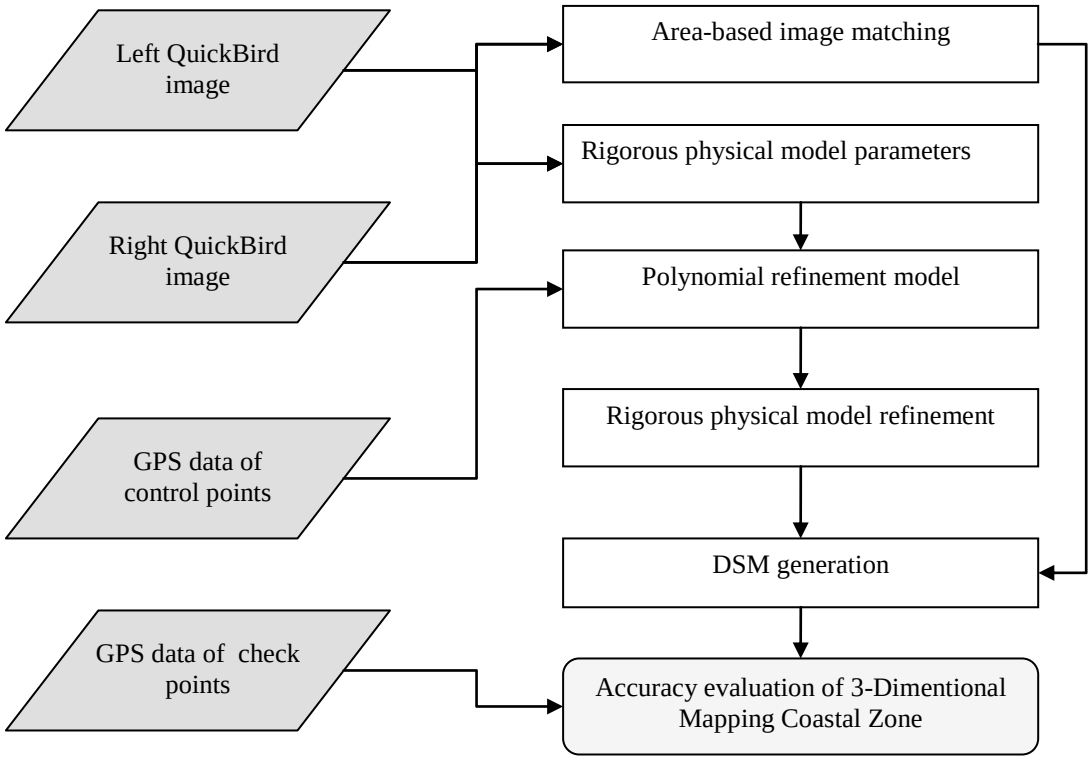

Figure 1.. Framework for 3-Dimentional Mapping Coastal Zone using QuickBird stereo images

2.1. Area-based Image matching

With the above stereo images, dense matching can be completed by using area image-matching procedure to match the respective images. Are-based image stereo matching [5] is a composite technique where first the similarity measure between template window and search window is found by normalized cross correlation technique. Least square also were used to improve the matching accuracy to sub-pixel. With this composite method dense point to point correspondence can be achieved with greater accuracy.

2.2. Rigorous physical model refinement

A rigorous sensor model (RPM) [3] is a physical model that describes the imaging geometry and the transformation between the object space and image space. For an image point within a CCD array, its image coordinates are (x_R , y_R) and ground coordinates (X_G , Y_G , Z_G). The coordinates of the

exposure centre of the array in the ground coordinate system at the imaging epoch t are (Xs(t), Ys(t), Zs(t)). Therefore, the collinearity condition [17] can be expressed as Equation (1):

$$x_R = z_R \frac{r_{11}(X_G - X_S(t)) + r_{12}(Y_G - Y_S(t)) + r_{13}(Z_G - Z_S(t))}{r_{31}(X_G - X_S(t)) + r_{32}(Y_G - Y_S(t)) + r_{33}(Z_G - Z_S(t))}$$
$$y_R = z_R \frac{r_{21}(X_G - X_S(t)) + r_{22}(Y_G - Y_S(t)) + r_{23}(Z_G - Z_S(t))}{r_{31}(X_G - X_S(t)) + r_{32}(Y_G - Y_S(t)) + r_{33}(Z_G - Z_S(t))} \quad (1)$$

And then, Incorporation of image polynomial terms into the basic model of Equation(1) yields a RPM refinement, which takes the form:

$$x_R = A_0 + A_1 x_R^{'} + A_2 y_R^{'} + A_3 x_R^{'} y_R^{'} + A_4 x_R^{'} x_R^{'} + \cdots = z_R \frac{r_{11}(X_G - X_S(t)) + r_{12}(Y_G - Y_S(t)) + r_{13}(Z_G - Z_S(t))}{r_{31}(X_G - X_S(t)) + r_{32}(Y_G - Y_S(t)) + r_{33}(Z_G - Z_S(t))} \quad (2)$$
$$y_R = B_0 + B_1 x_R^{'} + B_2 y_R^{'} + B_3 x_R^{'} y_R^{'} + B_4 y_R^{'} y_R^{'} + \cdots = z_R \frac{r_{21}(X_G - X_S(t)) + r_{22}(Y_G - Y_S(t)) + r_{23}(Z_G - Z_S(t))}{r_{31}(X_G - X_S(t)) + r_{32}(Y_G - Y_S(t)) + r_{33}(Z_G - Z_S(t))}$$

Where, ($x_R^{'}$, $y_R^{'}$) are image coordinate observations. $A_0 \cdots A_i$ and $B_0 \cdots B_i$ are the transformation parameters. Within this formulation there are four general logical choices of additional parameter (AP) sets: translation model, shift and drift model, affine model, second-order model and higher-order model. However, the reported results revealed that more than second-order model will perform unstable accuracy. Therefore, just former mentioned four refinement models will be used in this paper.

3. Experiment and discussion

3.1. Data Source

A basic QuickBird stereo pairs images were acquired on 2004 in Shanghai city and 73 RTK GPS-surveyed points were used to reconstruct the 3-Dimentional coastal zone.

3.2. Refinement accuracy

Owing to including systemic error about 10-25m in QuickBird image stereo position directly using the vender-provided RPMp, GCPs were added to reduce the systemic error and refined the RPMp. 29 well distributed control points were selected to refine the RPM p and the residual ground points as check points. The RMS errors were calculated in image space and the results indicated that the second-order polynomial refinement model obtained the best accuracy in east-west (RME:0.398m), south-north(RME:0.309) and elevation(RME:0.821m), respectively.

3.3. Three-Dimensional Mapping Coastal Zone

3-Dimentional Mapping Coastal Zone using QuickBird stereo images can be achieved by the framework showed in Fig.1. Figure 2 showed the proposed DSM created from QuickBird stereo image pairs. For checking the accuracy of created DSM, there were 44 ground points as check points for evaluation of the DSM accuracy. The RMS error showed on Table 1 was calculated and the RMS error reached 1.146m. However, the maximum residual of check points was 5.096m over four times of RMS error, which revealed that some error corresponding points remain in processing.

Table 1. Accuracy of CKPs of 3-Dimentinal Coastal Zone

DSM accuracy of CKPs	
Number of CKPs	44
Maximum residual (m)	0.025
Minimum residual (m)	5.096
Mean residual (m)	-0.024
RMS error (m)	1.146

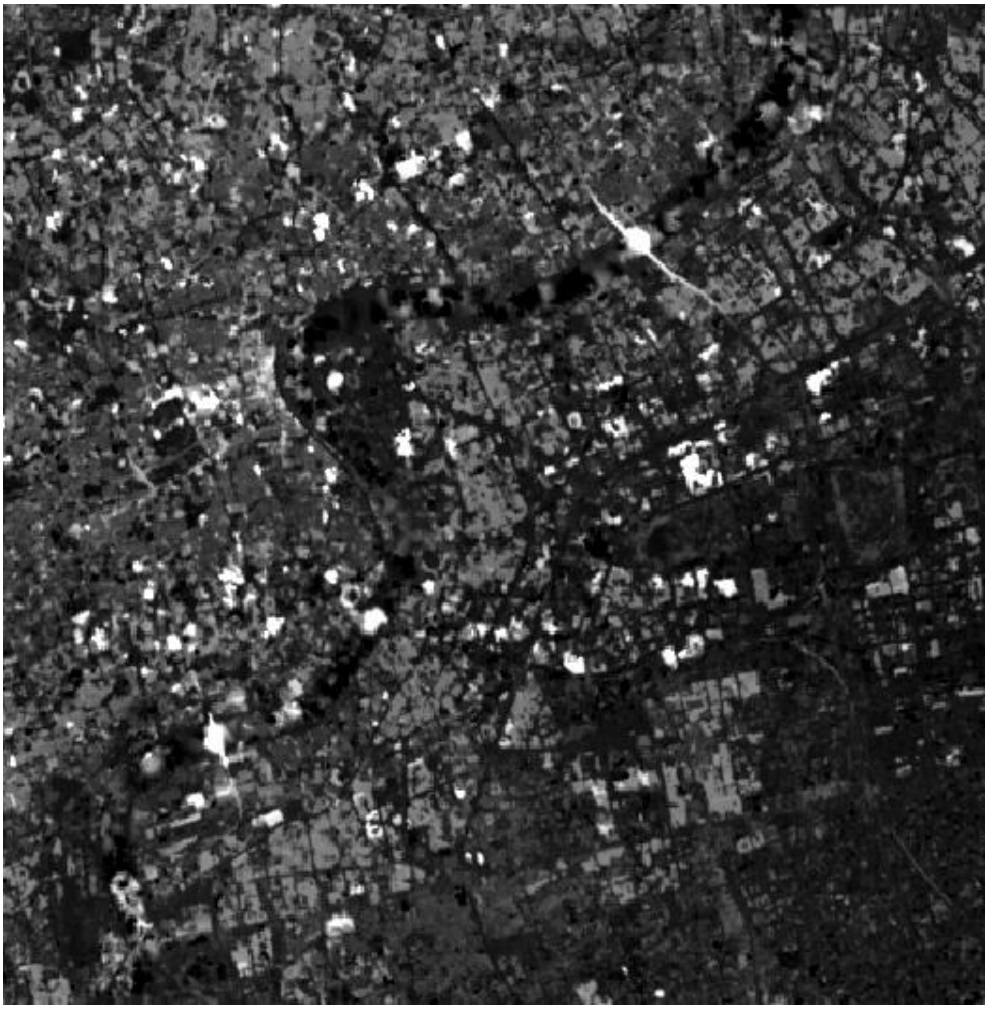

Figure 2. 3-Dimentional Mapping Coastal Zone using QuickBird stereo images

4. Conclusions and future works

In this report the RPM refinement applied and results of 3-Dimentional mapping coastal zone using QuickBird stereo images in Shanghai city, China are described. Owing to the bias errors in the vendor-provided RPMp with the QuickBird imageries, the second-order polynomial refinement model in the image space, which produced the 0.5m in horizontal direction and 0.8m in vertical direction accuracy, was adopted for the DSM generation. Future work will combine the optical and SAR images to reconstruct the 3-Dimentional mapping coastal zone.

5. References

[1] Aguilar M A, Aguilar F J, Agüera F and Sánchez J A 2007 Geometric accuracy assessment of QuickBird Basic Imagery using different operational approaches *Photogramm Eng Rem S* **12** 1321-1332.

[2] Capaldo P, Crespi M, Fratarcangeli F, Nascetti A and Pieralice F 2012 DSM generation from high resolution imagery applications with WorldView-1 and Geoeye-1 *Ita J. Remote Sens* **1** 41-53.

[3] Di K, Ma R and Li R 2003 Rational functions and potential for rigorous sensor model recovery, *Photogramm Eng Rem S* **1** 33-41.
[4] Fraser C S and Hanley H B 2005 Bias compensated RPCs for sensor orientation of high-resolution satellite imagery *Photogramm Eng Rem S* **8** 909-915.
[5] Joglekar J and S.Gedam S 2012 Area Based Image Matching Methods – A Survey *Int J. Emerg Tech Advanced Eng* **1** 130-136.
[6] Li R, Di K and Ma R 2003 3D shoreline extraction from Ikonos satellite imagery, The 4th Special Issue on Marine & Coastal GIS – *J. Mar Geod* **1/2** 107-115.
[7] Li R, Zhou F, Niu X and Di K 2007 Integration of Ikonos and QuickBird Imagery for geopositioning accuracy analysis *Photogramm Eng Rem S* **9** 1067-1074.
[8] Li R, Deshpande S, Niu X, Zhou F, Di K and Wu B 2008 Geometric Integration of Aerial and High-Resolution Satellite Imagery and Application in Shoreline Mapping *Mar Geod* **31** 143-159.
[9] Li R, Niu X, Liu C, Wu B and Deshpande D 2009 Impact of imaging geometry on 3D geopositioning accuracy of stereo IKONOS imagery *Photogramm Eng Rem S* **9** 1119-1125.
[10] Li X J and C.J.Damen M 2010 Coastline change detection with satellite remote sensing for environmental management of the Pearl River Estuary, China *J. Marine Syst* **82** S54-S61.
[11] Liu H X, Wang L, J. Sherman D, Wu Q S and Su H B 2011 Algorithmic Foundation and Software Tools for Extracting Shoreline Features from Remote Sensing Imagery and LiDAR Data *J. Geogr Inf Sys* **3** 99-119
[12] Poli D and Toutin T 2012 Review of developments in geometric modelling for high resolution satellite pushbroom sensors *Photogramm Rec* **27** 58-73
[13] Sesli F A, Karsli F, Colkesen I and Akyol N 2009 Monitoring the changing position of coastlines using aerial and satellite image data: an example from the eastern coast of Trabzon, Turkey *Environ Monit Assess* **1-4** 391-403
[14] Tong X H, Liu S J and Weng Q H 2010 Bias-corrected rational polynomial coefficients for high accuracy geo-positioning of QuickBird stereo imagery *ISPRS J. Photogramm* **2** 218-226
[15] Tong X H, Hong Z H, Liu S J, Zhang X, Xie H, Li Z Y, Yang S L, Wang W A and Bao F 2012 Building-damage detection using pre- and post-seismic high-resolution satellite stereo imagery : A case study of the May 2008 Wenchuan earthquake *ISPRS J. Photogramm* **2** 13-27
[16] Toutin, T., 2006. Comparison of 3D physical and empirical models for generating DSMs from stereo HR images *Photogramm Eng Rem S* **5** 597-604
[17] Zhou G and Li R 2000 Accuracy evaluation of ground points from Ikonos high-resolution satellite imagery *Photogramm Eng Rem S* **9** 1103-1112

Acknowledgments
Research supported by The Program for Professor of Special Appointment (Eastern Scholar) at Shanghai Institutions of Higher Learning, and supported by Shanghai Science and Technology Committee (Project 11510501300).